Human Molecular Genetics, 2010, Vol. 19, No. 11 **2239–2250**
doi:10.1093/hmg/ddq103
Advance Access published on March 10, 2010

Trafficking defects and loss of ligand binding are the underlying causes of all reported *DDR2* missense mutations found in SMED-SL patients

Bassam R. Ali[1,†], Huifang Xu[4,†], Nadia A. Akawi[1], Anne John[1], Noushad S. Karuvantevida[1], Ruth Langer[2], Lihadh Al-Gazali[3,†] and Birgit Leitinger[4,*,†]

[1]Department of Pathology, [2]Department of Radiology and [3]Department of Pediatrics, Faculty of Medicine and Health Sciences, United Arab Emirates University, Al-Ain, United Arab Emirates and [4]Molecular Medicine Section, National Heart and Lung Institute, Imperial College London, London SW7 2AZ, UK

Received February 2, 2010; Revised and Accepted March 4, 2010

Spondylo-meta-epiphyseal dysplasia (SMED) with short limbs and abnormal calcifications (SMED-SL) is a rare, autosomal recessive human growth disorder, characterized by disproportionate short stature, short limbs, short broad fingers, abnormal metaphyses and epiphyses, platyspondyly and premature calcifications. Recently, three missense mutations and one splice-site mutation in the *DDR2* gene were identified as causative genetic defects for SMED-SL, but the underlying cellular and biochemical mechanisms were not explored. Here we report a novel *DDR2* missense mutation, c.337G>A (p.E113K), that causes SMED-SL in two siblings in the United Arab Emirates. Another *DDR2* missense mutation, c.2254C>T (p.R752C), matching one of the previously reported SMED-SL mutations, was found in a second affected family. DDR2 is a plasma membrane receptor tyrosine kinase that functions as a collagen receptor. We expressed DDR2 constructs with the identified point mutations in human cell lines and evaluated their localization and functional properties. We found that all SMED-SL missense mutants were defective in collagen-induced receptor activation and that the three previously reported mutants (p.T713I, p.I726R and p.R752C) were retained in the endoplasmic reticulum. The novel mutant (p.E113K), in contrast, trafficked normally, like wild-type DDR2, but failed to bind collagen. This finding is in agreement with our recent structural data identifying Glu113 as an important amino acid in the DDR2 ligand-binding site. Our data thus demonstrate that SMED-SL can result from at least two different loss-of-function mechanisms: namely defects in DDR2 targeting to the plasma membrane or the loss of its ligand-binding activity.

INTRODUCTION

The discoidin domain receptors (DDRs), DDR1 and DDR2, comprise a family of receptor tyrosine kinases (RTKs) that function as collagen receptors (1,2). The DDRs are the only RTKs that are activated by a component of the extracellular matrix. Several collagen types, both fibrillar and non-fibrillar types, activate the DDRs, with the two receptors displaying different specificities for certain collagen types (1–4). Structurally, the DDRs are characterized in their extracellular regions by the presence of a collagen-binding discoidin homology domain and a domain unique to the DDRs (stalk region) (Fig. 1). A transmembrane region is followed by a large cytoplasmic juxtamembrane domain, and, finally a C-terminal tyrosine kinase domain. Both DDRs form ligand-independent dimers on the cell surface (5). We have recently defined the mode of collagen recognition by the discoidin domain of DDR2 using X-ray crystallography (6).

The DDRs control fundamental cellular processes including cell proliferation, adhesion and migration (7,8). In addition,

*To whom correspondence should be addressed at: Molecular Medicine Section, NHLI, Imperial College London, Sir Alexander Fleming Building, London SW7 2AZ, UK. Tel: +44 2075941591; Fax: +44 2075943100; Email: b.leitinger@imperial.ac.uk
†The authors wish it to be known that, in their opinion, the first two authors should be regarded as joint first authors and the last two authors should be regarded as joint senior authors.

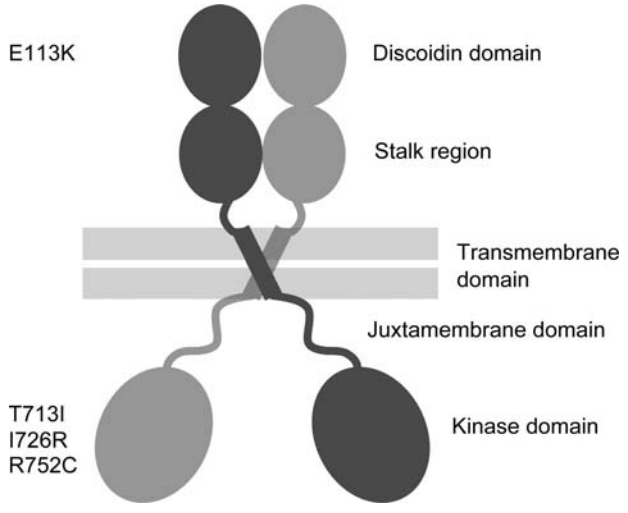

Figure 1. Schematic domain structure of homodimeric DDR2. The extracellular domain consists of a collagen-binding discoidin domain, followed by a so-called stalk region. The intracellular domain contains a large cytosolic juxtamembrane domain in addition to the C-terminal tyrosine kinase domain. The position of disease-causing missense mutations is shown at the left.

the DDRs regulate extracellular matrix remodeling by controlling matrix metalloproteinase expression and activity. Both receptors are associated with human diseases, including fibrotic disorders of the lung (DDR1), liver (DDR2) and kidney (DDR1); atherosclerosis (DDR1); osteoarthritis (DDR2); rheumatoid arthritis (DDR2); and several types of malignancies (7).

DDR2, like DDR1, is widely expressed in different tissues during development and in postnatal tissues (7). While DDR1 is mostly confined to epithelial cells and leukocytes, DDR2 is found on cells of mesenchymal origin. Mice lacking DDR2 exhibit dwarfism (9,10), indicating that DDR2 plays an important role in bone growth. Labrador *et al*. (9) showed that targeted deletion of *Ddr2* in mice led to shortened long bones due to reduced chondrocyte proliferation. In another study, Kano *et al*. (10) characterized a spontaneously occurring, autosomal-recessive mutation in their mouse colony that led to a 150 kb deletion encompassing the first 17 exons of the *Ddr2* gene. These latter mice, termed *slie* mutant mice, were infertile in addition to being dwarfed (10).

Recently, DDR2 function has been implicated in human skeletal growth. Three *DDR2* gene missense mutations and one splice site mutation were each shown to cause spondylometa-epiphyseal dysplasia (SMED) with short limbs and abnormal calcifications [SMED-SL (MIM 271665)] (11). SMED-SL is a rare, autosomal recessive, human growth disorder. Patients exhibit normal intelligence, disproportionate short stature, platyspondyly, abnormal epiphyses and metaphyses, narrow chest, shortening of the lower and upper limbs, short broad fingers and premature calcifications (12,13).

DDR2 is a member of the subfamily of RTKs that also include ROR2. Mutations in the *ROR2* gene have been shown to be the underlying cause of the recessive form of Robinow Syndrome, a skeletal dysplasia characterized by short stature, limb shortening, genital hypoplasia and craniofacial abnormalities (14). We have recently shown that all the missense pathogenic mutations in ROR2 are retained in the endoplasmic reticulum (ER) and are substrates for the ER quality control system, demonstrating that ER retention is the underlying cellular mechanism of this condition (15,16) (Ali *et al*., unpublished data). Given the phylogenetic relatedness of DDR2 to ROR2, we reasoned that most SMED-SL causing missense mutations in DDR2 are likely to result in the retention of DDR2 protein in the ER. In addition, patients with SMED-SL phenotype have been reported in the United Arab Emirates (UAE), but the molecular defects responsible for their symptoms have not been established (17) (Al-Gazali *et al*., unpublished data). In this article, we report the evaluation of two families from the UAE with SMED-SL and the identification of two mutations including a novel missense mutation in DDR2. In addition, we report the elucidation of the cellular and biochemical mechanisms of all the missense mutations so far found in patients with this condition. While the previously established SMED-SL DDR2 mutations indeed caused ER retention of mutated DDR2, we demonstrate that the novel SMED-SL mutation (p.E113K) resulted in a ligand-binding defect. These latter data fit well with our recent structural data on the ligand-binding site of DDR2 (6). Furthermore, our data demonstrate further the widespread involvement of the ER quality control systems in the cellular mechanisms of numerous secretroy pathway targeted proteins (15,18–20).

RESULTS

Clinical characteristics of patients with SMED-SL from United Arab Emirates

Two consanguineous families with SMED-SL from the UAE have been evaluated (see Supplementary Material, Fig. S1 for the pedigrees). The first is a Pakistani family with two affected children. The clinical details of the affected children are described in detail below. The second family is of Egyptian background with two affected children and was described in detail before (17). The family was found to have the same mutation, c.2254C>T (p.R752C), as found in the Palestinian families described by Bargal *et al*. (11). The severity of the clinical features in this family, particularly the degree of chondral calcifications, was also similar to the clinical features of the families described by Bargal *et al*. (11). Both children in this family died, one at the age of 13 years due to respiratory complications and the other one died suddenly at 8 years of age due to cord compression.

Family 1, Case 1. This male child was the product of normal pregnancy. Delivery at term was by lower section Cesarean section. Prenatal ultrasound showed short limbs and short stubby hands. His birth weight was 2700 gm (5%) and length was 47 cm (10%). At birth, he was noted to have in addition to the short limbs and short hands, bowing of the lower limbs. The diagnosis of achondroplasia was suggested. During the first year of life and the early childhood years, he had repeated chest infections which were not severe enough to require hospital admissions. These attacks got better with time and stopped when he was 6 years old. His early developmental milestones were normal. He was operated on both legs to correct the bowing. He was evaluated by us at the age of 9.5 years. His weight was 27.5 kg (10%) and height was 99 cm ($\ll < 3\%$, -6 SD). He had dysmorphic features

Table 1. Clinical features of the two new cases compared to the literature (11–13,17,31–34)

Features	Case 1	Case 2	Literature (24 cases)
Clinical			
Short limbs	+	+	24/24
Short broad hands	+	+	24/24
Short puffy fingers	+	+	10/24
Bowing of legs	+	+	7/24
Narrow chest	−	+	18/24
Pectus excavatum	−	+carinatum	8/24
Respiratory problems	Mild	Mild	12/24
Hypertelorism	+	+	20/24
Short flat nose	+	+	21/24
Wide nostril	−	−	18/24
Long philtrum	−	−	18/24
Short neck	+	+	8/24
Neck hyperextension	−	−	4/24
Peculiar voice	+	−	5/23
Delayed motor development	−	−	17/24
Delayed mental development	−	−	4/24
Radiological			
Short and broad long bones	+	+	24/24
Short and broad round bones	+	+	24/24
Abnormal metaphyses & epiphyses	+	+	24/24
Rib abnormalities	+	+	24/24
Chondral calcification	+ (minimal)	+ (minimal)	10/24
Platyspondyly	+	+	24/24
C1–C2 instability	−	−	13/24

and shortening of all limbs with very short puffy hands (Table 1). He was attending normal school at the appropriate grade and was top of the class. Neurological examination was normal. Skeletal survey revealed changes typical of SMED-SL including short and broad long bones with irregular flared metaphyses of the proximal and distal ends and genu varum (Table 1). There was a small thoracic diameter with short and broad ribs with very few calcifications at the costochondral margin (Fig. 2A).

Family 1, Case 2. Brother of case 1, the product of normal pregnancy and term delivery by LCS. His weight was 2.9 kg (10%) and length was 49 cm (25%). Short limbs and short hands were diagnosed prenatally. He was found to have bowing of limbs in addition to the shortening. He had, similar to his brother, repeated respiratory infections not requiring hospital admissions. He was evaluated by us at 8 years of age. His weight was 17.6 kg (<5%) and height was 94 cm (<3%, −6 SD). He had similar dysmorphic features as his brother but his chest appeared much narrower than his brother's. He was attending normal school at the appropriate grade and was top of the class. Neurological examination was normal. Skeletal survey revealed similar changes to his brother (Fig. 2B and Table 1).

Molecular analysis reveals that SMED-SL in families from the UAE is caused by two missense mutations in DDR2

The genomic DNA from SMED-SL affected individuals and their parents (Supplementary Material, Fig. S1) was isolated and all the exons and flanking regions of the *DDR2* gene were amplified by PCR as described in the Materials and Methods. Direct DNA sequencing revealed two homozygous missense mutations: c.337G>A (p.E113K) for family 1 and c.2254C>T (p.R752C) for family 2 (Supplementary Material, Fig. S2). The parents in each case were heterozygous for the mutation found in their affected offspring. The nucleotide change c.337G>A has not been found in 100 ethnically matched controls. In addition, the p.E113K mutation is novel and is located in the ligand-binding domain of the DDR2 protein (Fig. 1). The amino acid change is physiochemically significant (a change of the negatively charged glutamic acid to the positively charged lysine) and affects an important residue within the discoidin domain, the DDR2 ligand-binding domain (6). Furthermore, this residue is conserved in the DDR2 protein from different species including zebrafish, mouse and human (Supplementary Material, Fig. S3). These pieces of data together with the functional assays described below confirm the pathogenicity of this amino acid substitution. On the other hand, the mutation (p.R752C) found in the family of Egyptian origin is a recurring mutation and has been recently found as a founder mutation in five Palestinian families from Jerusalem (11). This mutation is located in the DDR2 intracellular domain, as shown in Figure 1.

SMED-SL missense mutations p.T713I, p.I726R and p.R752C lead to loss of plasma membrane expression of DDR2 and accumulation in the endoplasmic reticulum, while the p.E113K mutant exhibits similar subcellular localization as the wild-type protein

We hypothesized that most of the missense mutations in DDR2 (Fig. 1) will result in the retention of the mutated protein in the ER. This assumption was based on the relatedness of DDR2 to ROR2 and our findings that all the pathogenic missense mutations in ROR2 have been shown to be retained in the ER (15,16). Therefore, we generated all the missense mutations found in SMED-SL patients including

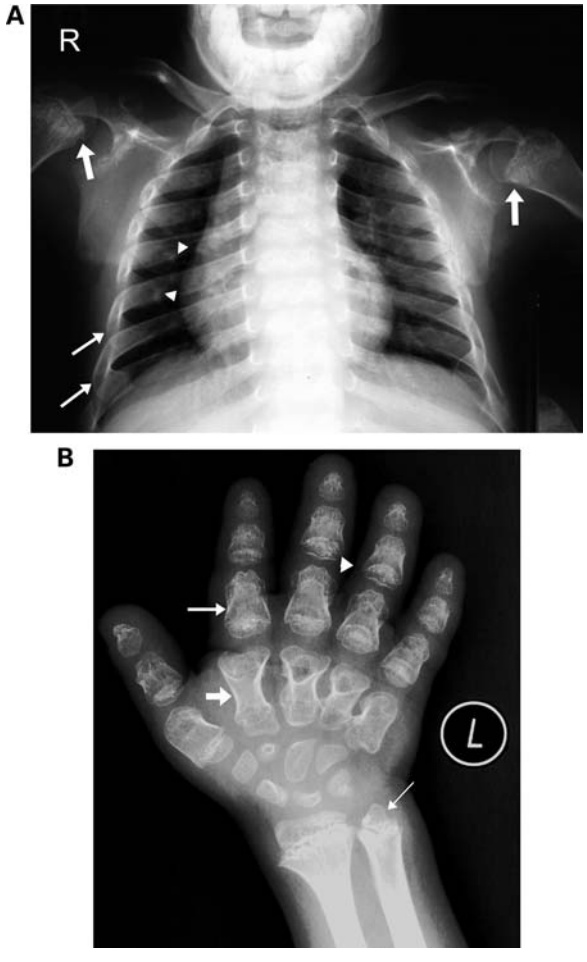

Figure 2. Chest and hand radiographs of cases 1 and 2. (**A**) Chest radiograph of case 1 at 9.5 years. Narrow thorax with short broad ribs, more at the lateral and anterior aspects (thin arrows) than at the costo-vertebral joints. Note very few calcifications at the costal cartilage on the right side (arrow heads). Note also irregularities at the humeral meta/epiphyses with calcifications (thick arrows). (**B**) Radiograph of the left hand (dorso-volar projection) of case 2 at 8 years of age showing short and broad tubular bones with typical diaphyseal constriction (medium arrow). The metacarpal bones are narrower at the proximal end giving the appearance of drumsticks (thick arrow). There is some bone-within-bone appearance of the phalanges (medium arrow). The distal phalanges are triangular in shape. The epiphyses of the phalanges appear irregular and cone-shaped (arrow head). Small and irregular precocious carpal bones. The distal metaphyses of the radius and ulna is broad and irregular with irregular trabecular structure. The distal ulnar epiphysis is triangular in shape (thin arrow).

those reported by Bargal *et al*. (11) in a mammalian expression system using site-directed mutagenesis and expressed the proteins in HeLa cells as described in the Materials and Methods. Confocal microscopy imaging revealed that the C-terminally HA-tagged wild-type DDR2 protein was primarily localized to the cell surface and colocalized with the plasma membrane marker GFP-h-Ras (Fig. 3A–C). We also observed some intracellular staining of the wild-type protein which presumably represents the newly synthesized protein that is in transit to the cell surface. Similarly, the p.E113K mutant was located to the periphery of the cell and colocalized with GFP-h-Ras (Fig. 3D–F). In contrast, confocal imaging of p.T713I, p.I726R and p.R752C mutants revealed an intracellular and reticular localization of the proteins, which is clearly different from that of the wild-type protein, with no colocalization with the plasma membrane marker (Fig. 3G–O). This intracellular staining is reminiscent of ER staining and we therefore co-stained cells expressing the wild-type and mutant proteins with a well established ER marker (calnexin). As shown in Figure 4A–F, the wild-type protein and p.E113K mutant showed distinct and different localizations from that of calnexin, confirming plasma membrane locations. On the other hand, the three intracellular missense mutants (p.T713I, p.I726R and p.R752C) showed a high degree of colocalization with the ER marker (Fig. 4G–O) indicating ER localization. Further biochemical studies (the following sections) confirmed the ER localization of the three proteins.

Lack of collagen-induced transmembrane signaling is due to trafficking defects of the DDR2 mutants p.T713I, p.I726R and p.R752C. The first step in collagen-induced DDR2 transmembrane signaling is activation of DDR2, which manifests itself in autophosphorylation of cytoplasmic tyrosine residues (1,2). To analyze whether SMED-SL disease mutants could be activated by binding to collagen, we transiently expressed the mutants and wild-type DDR2 in HEK293 cells. HEK293 cells were chosen for these experiments, as DDR autophosphorylation in these cells can be easily monitored by western blotting of cell lysates (1,21). In transfected HEK293 cells, wild-type DDR2 is usually observed as a mixture of three (sometimes four) molecular weight forms between ~125 and 130 kDa (5,21,22), with the upper forms representing complex glycosylated mature forms. Unlike wild-type DDR2, however, for which the expected molecular weight forms were detected (Fig. 5A), the SMED-SL mutants p.T713I, p.I726R and p.R752C were detected predominantly as the lowest molecular weight species (Fig. 5A), with mutants p.T713I and p.I726R displaying a small amount of the middle forms. None of these mutants displayed the highest molecular weight form of DDR2. In addition, Endo H treatment of cell lysates expressing wild-type or mutant DDR2 showed that the predominant forms of T713I-DDR2, I726R-DDR2 and R752C-DDR2 were sensitive to Endo H digestion, as was the lowest molecular weight form of wild-type DDR2 (Fig. 5A), suggesting that these molecular weight species represent immature biosynthetic precursors of DDR2. This is in agreement with the protein localization data in HeLa cells, presented in Figures 3 and 4. The predominant forms of wild-type DDR2, however, were the upper molecular weight species, which were largely absent in the mutant receptors. These forms were Endo H resistant and thus represent the complex glycosylated mature forms of DDR2.

As expected, a strong collagen-induced phosphorylation signal was observed for the upper forms of wild-type DDR2 (Fig. 5B, upper blot lanes 1 and 2). In keeping with the lack of plasma membrane localization of T713I-DDR2, I726R-DDR2 and R752C-DDR2, no collagen I-induced phosphorylation could be detected for any of these mutant receptors (Fig. 5B, upper blot lanes 3–7).

Loss of E113K-DDR2 transmembrane signaling despite normal cellular trafficking. In contrast to mutants T713I-DDR2, I726R-DDR2 and R752C-DDR2, which displayed

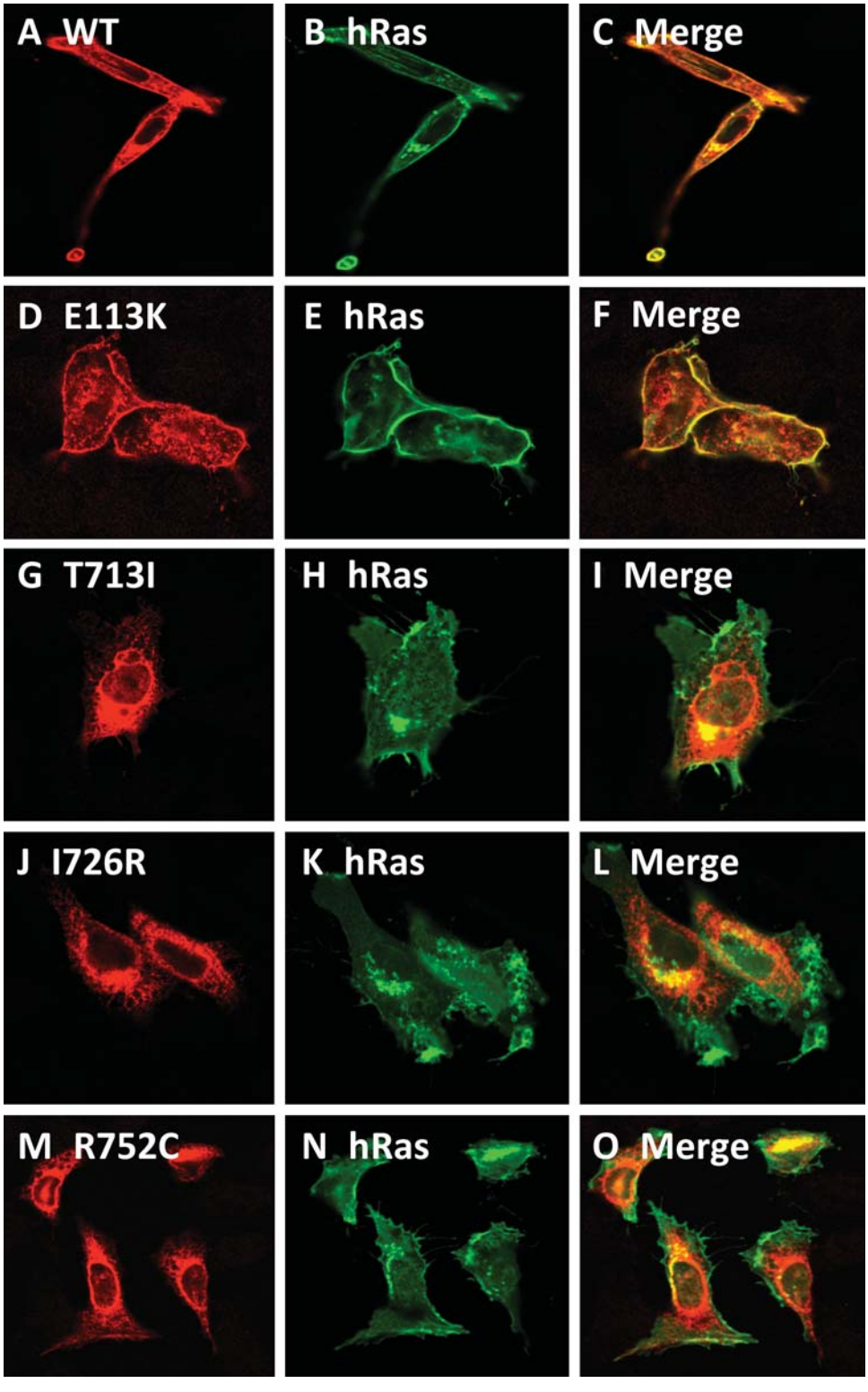

Figure 3. Comparison of subcellular localization of DDR2 wild-type and SMED-SL patient mutant variants. HeLa cells were transiently co-transfected with plasmids encoding the indicated HA-tagged DDR2 protein and EGFP-tagged H-Ras, fixed and stained with anti-HA antibodies as described in Materials and Methods. (**A**), (**D**), (**G**), (**J**) and (**M**) show the distribution of over-expressed HA-tagged DDR2 proteins. (**B**), (**E**), (**H**), (**K**) and (**N**) show the distribution of over-expressed EGFP-tagged H-Ras, which is predominantly localized to the plasma membrane, while (**C**), (**F**), (**I**), (**L**) and (**O**) show the extent of co-localization of DDR2 proteins with EGFP-H-Ras.

predominant ER localization, E113K-DDR2 was found on the plasma membrane in HeLa cells (Figs 3 and 4). Transient expression of E113K-DDR2 in HEK293 cells resulted in the appearance of the same molecular weight forms as observed for wild-type DDR2, with only the lowest molecular weight form showing sensitivity to Endo H treatment (Fig. 6A). The upper

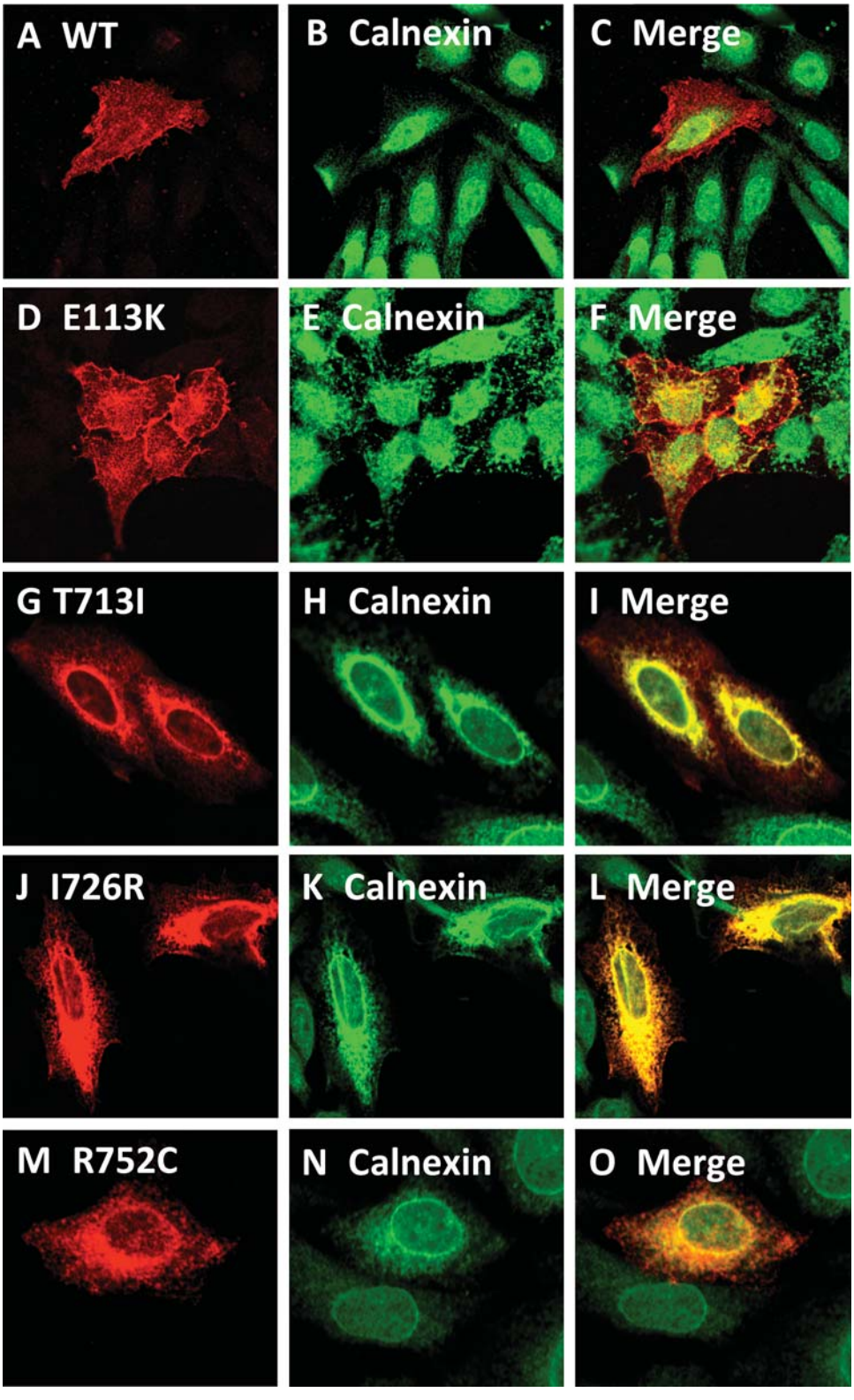

Figure 4. Comparison of the intracellular localization of DDR2 wild-type and SMED-SL patient mutant variants with the ER marker. HeLa cells were transiently transfected with plasmids encoding the indicated HA-tagged DDR2 protein, fixed and stained with antibodies against the HA-tag (monoclonal) and calnexin (polyclonal) as described in Materials and Methods. (**A**), (**D**), (**G**), (**J**) and (**M**) show the distribution of over-expressed HA-tagged DDR2 proteins. (**B**), (**E**), (**H**), (**K**) and (**N**) show the distribution of calnexin, which is predominantly localized to the ER, while (**C**), (**F**), (**I**), (**L**) and (**O**) show the extent of co-localization of DDR2 proteins with calnexin.

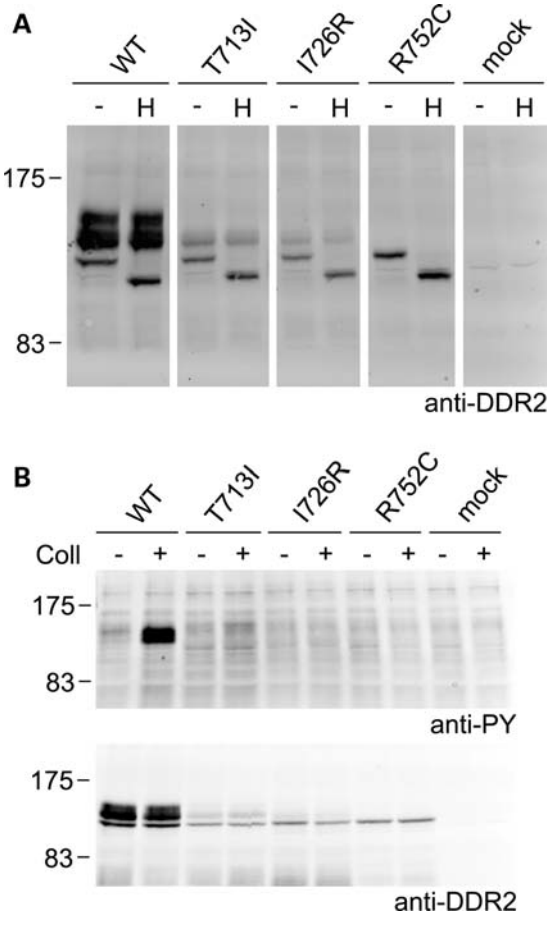

Figure 5. Defective cellular trafficking causes loss of collagen-induced signaling for the SMED-SL patient mutant variants T713I-DDR2, I726R-DDR2 and R752C-DDR2. HA-tagged full-length DDR2 wild-type or mutant variants were transiently expressed in HEK293 cells. (**A**) Cell lysates were treated with Endoglycosidase H for 3 h at 37°C (*H*) or left untreated for 3 h at 37°C (−) and analyzed by SDS–PAGE and western blotting. The blot was probed with polyclonal anti-DDR2 antibodies. (**B**) Cells were stimulated with 10 μg/ml of rat tail collagen I (+) or 1 mM acetic acid (−) for 90 min at 37°C. Cell lysates were analysed by SDS–PAGE and western blotting. The blots were probed with anti-phosphotyrosine (anti-PY) monoclonal antibody 4G10 (upper blot) or polyclonal anti-DDR2 antibodies (lower blot). The positions of molecular markers (in kDa) are indicated. The experiments were carried out three times with very similar results.

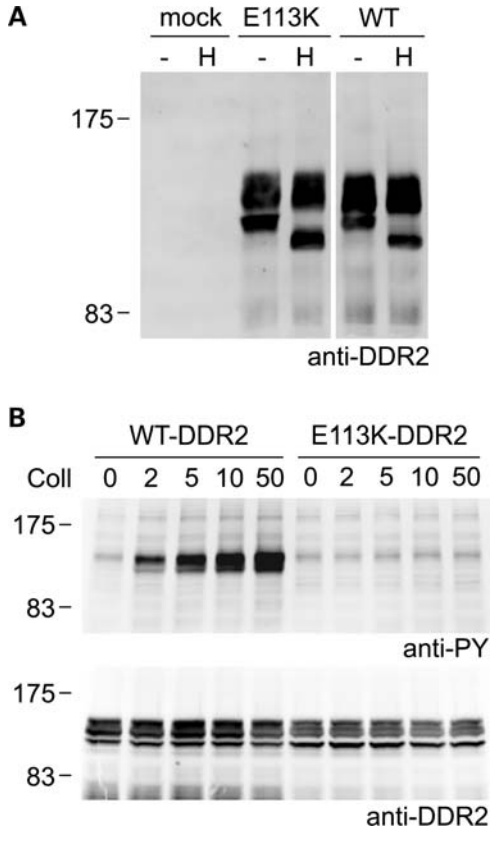

Figure 6. Loss of collagen-induced signaling despite normal cellular trafficking of E113K-DDR2. Untagged full-length DDR2 wild-type or E113K-DDR2 were transiently expressed in HEK293 cells. (**A**) Cell lysates were treated with Endoglycosidase H for 3 h at 37°C (*H*) or left untreated for 3 h at 37°C (−) and analyzed by SDS–PAGE and western blotting. The blot was probed with polyclonal anti-DDR2 antibodies. (**B**) Cells were stimulated for 90 min at 37°C with rat tail collagen I at the indicated concentrations (in μg/ml). Cell lysates were analyzed by SDS–PAGE and western blotting. The blots were probed with anti-phosphotyrosine (anti-PY) monoclonal antibody 4G10 (upper blot) or polyclonal anti-DDR2 antibodies (lower blot). The positions of molecular markers (in kDa) are indicated. The experiments were carried out three times with very similar results.

species of E113K-DDR2 are thus complex glycosylated and likely represent mature forms of the receptor. Unlike wild-type DDR2, however, E113K-DDR2 could not be activated by collagen I. Even at high concentrations of collagen I (50 μg/ml), no collagen I-induced phosphorylation signal was detected (Fig. 6B), indicating that plasma-membrane localized E113K-DDR2 is defective in transmembrane signaling.

Loss of ligand binding of E113K-DDR2. We recently identified glutamate 113 as one of the major collagen-binding residues in DDR2 (6). Glu113 forms a salt bridge with Arg105 in the DDR2 discoidin domain. Substitution of the glutamate by lysine would disrupt the salt bridge and is expected to negatively impact on ligand binding by E113K-DDR2. To analyze the effect of p.E113K substitution on DDR2 collagen binding, we created a soluble ectodomain construct with the p.E113K mutation and expressed it in HEK293-EBNA cells. This construct was secreted at similar levels to the corresponding wild-type protein, indicating that the mutation did not result in gross abnormalities of protein folding. The mutant protein failed to bind to collagens types I and II in an established solid-phase binding assay, displaying similar low-level binding to a DDR2 variant harboring the p.W52A mutation (Fig. 7B and C). We and others recently showed that Trp52, like Glu113, plays a critical role in collagen recognition by DDR2, and that substitution of Trp52 by Ala abolishes collagen I and collagen II binding (6,23). We conclude that substitution of Glu113 by Lys leads to loss of ligand binding, which in turn is responsible for lack of collagen-induced signaling of full-length E113K-DDR2.

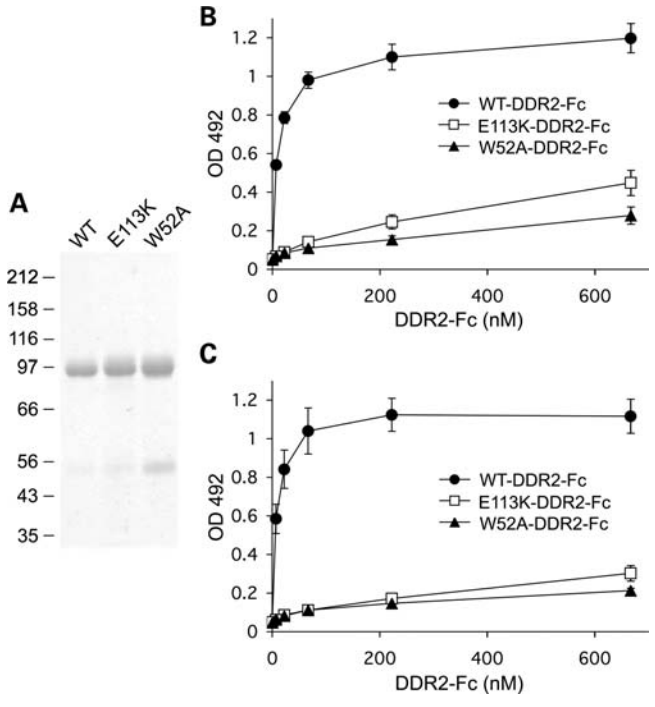

Figure 7. Loss of collagen-binding function of E113K-DDR2. (**A**) SDS–polyacrylamide gel electrophoresis of purified WT-DDR2-Fc, E113K-DDR2-Fc and W52A-DDR2-Fc. A Coomassie-blue-stained gel (7.5% gel) is shown. The positions of molecular weight markers (in kDa) are indicated. (**B** and **C**) Solid phase binding assays with recombinant wild-type DDR2-Fc, E113K-DDR2-Fc or W52A-DDR2-Fc. Recombinant DDR2 ectodomain proteins were added for 3 h at room temperature to 96-well plates coated with collagen I (B) or collagen II (C) at 10 μg/ml. Shown are the means ± SEM of three independent experiments, each performed in duplicates.

DISCUSSION

Here we report the clinical features of two siblings diagnosed with SMED-SL and a novel *DDR2* missense mutation identified in these patients. This mutation (p.E113K) is located in the extracellular discoidin domain and affects a surface-exposed residue that was previously identified as an important amino acid in the collagen-binding site of DDR2 (6,23). Additionally, we identified another mutation (p.R752C) in an Egyptian family with SMED-SL. This DDR2 mutation, localized in exon 17 of the *DDR2* gene, which encodes part of the intracellular tyrosine kinase domain, is a recurring mutation previously found in five Arab families from Jerusalem affected with SMED-SL (11).

Here we demonstrate the effects of all known SMED-SL causing missense mutations on DDR2. Our cellular and biochemical analysis of these four DDR2 mutations showed that these fall into two classes: all previously identified missense mutations cause a trafficking defect with the affected proteins mis-localizing to the ER, while the novel p.E113K-DDR2 mutation is localized in the cell similar to wild-type DDR2 but is defective in transmembrane signaling due to a ligand-binding defect. A previous report identified mutations in the *DDR2* gene as causative genetic defects for SMED-SL (11), but did not illuminate the mechanism of disease. Bargal *et al.* (11) speculated on the possible biochemical consequences of the disease mutations p.T713I, p.I726R and p.R752C. Because the affected amino acids are located in the active site of the DDR2 kinase, it was proposed that the substitutions may influence the stability of the activation loop, ATP binding affinity or substrate specificity, respectively (11). The possibility that protein folding may be affected was not considered. DDR2 is a member of the RTK family of plasma membrane receptors and is phylogenetically related to ROR2 (24). Missense mutations in the *ROR2* gene were recently shown to cause retention of the mutated proteins in the ER as a result of the protein folding quality control within this organelle named ER-Associated Protein Degradation (ERAD) (15,16). ERAD ensures that only properly folded proteins and fully assembled complexes are allowed to exit the ER to their final destinations. Proteins that fail to attain the required functional native conformations due to mutations or failure to acquire the needed posttranslational modifications, such as proteolytic cleavage of signal peptides, glycosylation and GPI-anchoring, are retained in the ER for a short period of time but then get targeted for re-translocation to the cytoplasm and degradation by the ubiquitin/proteasome systems (25–29).

In this report, we show that three out of four missense mutations (p.T713I, p.I726R and p.R752C) found in SMED-SL patients result in the retention of the affected proteins in the ER. ER retention of the three mutants is strongly supported by the confocal images presented in Figures 3 and 4 and the biochemical findings on the sensitivity to Endo H treatment presented in Figure 5. We noticed lower levels of expression of the ER-retained mutant proteins in HEK293 cells, compared with wild-type DDR2, as can be seen in Figure 5B. These low steady-state levels of the mutant proteins may be due to ERAD degradation. Additionally, our findings add another genetic condition to the 60 or so known to be caused by ERAD (15,18,19,30).

Unlike the ER-retained mutant DDR2 receptors, E113K-DDR2 was found at the cell surface, similar to wild-type DDR2 (Fig. 3A–F), indicating a different disease-causing mechanism. Glu113 is located in the DDR2 extracellular discoidin domain. The DDR2 discoidin domain adopts a β-barrel structure consisting of eight β-strands (23). At the top of the barrel, five protruding loops create a trench that forms the collagen-binding site (6,23). Glu113, which forms a salt bridge with Arg105, is one of several key residues that contact collagen (6). Figure 8, which shows a cartoon drawing of the DDR2 discoidin domain bound to a collagen peptide, illustrates how Glu113 is involved in the DDR2-collagen interaction. Data presented in Figure 7 demonstrate that E113K-DDR2 had lost most of the collagen-binding activity. This result agrees well with the previous observation that mutation of E113Q reduced collagen-binding to ∼10% of wild-type DDR2 (23). Thus, Glu113 is one of the main DDR2 residues contributing to collagen-binding. It is also noted that Glu113 and Arg105 are conserved in DDR1, further underscoring the importance of the Glu113-Arg105 salt bridge in the DDR-collagen interaction. This is the first report on the clinical relevance of substitutions at this site.

We noted some variations in the phenotype between the two families we are reporting here. For example, the clinical phenotype and the degree of chondral calcification of the second family (mutation p.R752C) were very severe (17). Both children had extensive calcifications which appeared by 1 years

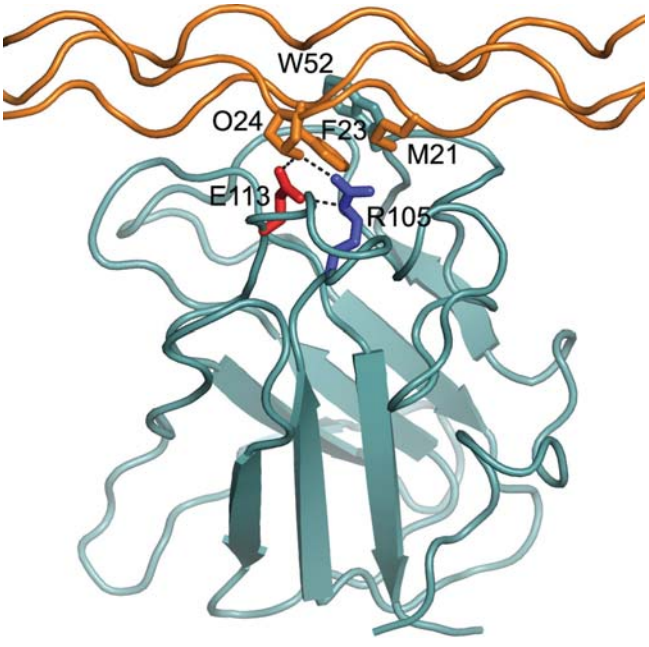

Figure 8. Cartoon drawing of the DDR2 discoidin domain (selected side chains: W52, cyan; R105, blue; E113, red) bound to a collagen peptide (selected side chains: M21 and O24 of leading chain, F23 of middle chain). Hydrogen bonds involving E113 are shown as dashed black lines. The Figure was prepared using the coordinates of PDB entry 2WUH (6).

of age and were very progressive and widespread involving almost all cartilages. In addition, both children had repeated respiratory infections requiring hospital admissions and leading to death in the older child. The younger sib had in addition symptoms of cord compression, which led to his sudden death. The phenotype in the affected children from the first family (mutation p.E113K), on the other hand, was less severe with very few mild respiratory infections not requiring hospital admissions. In addition, the chondral calcification was limited and much less severe than in the p.R752C family. This variability might be due to retention of some residual activity in the p.E113K mutant compared with the p.R752C mutant. Alternatively, cells expressing the ER-retained mutated protein (p. R752C) may experience ER stress, which would not be experienced by cells expressing the correctly targeted p.E113K protein. However, the clinical significance of these presumed differences in ER stress responses are unknown at this stage.

How does DDR2 control bone growth? Very little is known about the role of DDR2 in bone growth. DDR2 is expressed on chondrocytes and its elimination in the mouse leads to suppression of chondrocyte cell proliferation (9). It is assumed that the interaction of DDR2 with collagen II in the proliferative zone of the growth plate is responsible for controlling chondrocyte proliferation. DDR2 is also a receptor for another collagen type with relevance to bone growth, collagen X (4). While collagen II is found in all types of cartilage, collagen X expression is restricted to the hypertrophic zone of the growth plate. We show here that E113K-DDR2 is unable to interact with collagen II (Fig. 7C). Further studies are required to establish whether the mutant protein is also defective in binding to collagen X.

In mice with targeted DDR2 deletion, the growth plates were observed to be shortened (9). In the only available histological study of a chostrochondral junction from a SMED-SL patient, extremely abnormal cartilage was found (12). The growth plate was found to lack proliferating chondrocyte columns. Chondrocytes were small and sparse in the resting zone, often surrounded by a 'ring-like' amorphous matrix, which in turn could be surrounded by a more densely packed structure of fibrillar collagen. Clustering of chondrocytes within lacunae was also observed. Taken together with our data, it can be speculated that in SMED-SL patients, lack of DDR2 interaction with collagen II results in impaired DDR2 signaling, leading to severe suppression of chondrocyte proliferation, which may be responsible for poor linear bone growth. Further morphological studies on patient samples with known DDR2 mutations would be required to confirm this hypothesis.

In summary, we report a novel mutation in the *DDR2* gene in patients affected with SMED-SL and elucidate the cellular and biochemical mechanisms underlying all reported SMED-SL disease mutations. Two different mechanisms, failure to reach the plasma membrane and impaired ligand binding, were found to result in the growth disorder. This study supports the notion that DDR2 signaling is important in human development and that the interaction of DDR2 with collagen is essential for proper skeletal growth.

MATERIALS AND METHODS

Patients

The research was approved by Al-Ain Medical District Human Research Ethics Committee and informed consent was obtained from the parents. Patients were evaluated by a clinical geneticist and their radiography imaging were also evaluated.

Chemicals and reagents

Bovine serum albumin was obtained from Fisher Scientific (Loughborough, UK). Collagen I (acid-soluble from rat tail; C-7661) was purchased from Sigma (Poole, UK). Bovine collagen II, ELISA grade, was from Chondrex Inc. (Redmond, WA, USA). Endoglycosidase H (Endo Hf) was purchased from New England Biolabs (Hertfordshire, UK). The antibodies and their sources were as follows: antibodies for immunofluorescence: mouse anti-HA-Tag monoclonal antibody (dilution 1:200; Cell Signaling Technology), rabbit anti-calnexin polyclonal antibody (dilution 1:500; StressGen Biotechnologies), Alexa Fluor 568-goat anti-mouse IgG (dilution 1:200; Molecular Probes), Alexa Fluor 488-goat anti-rabbit IgG (dilution 1:200; Molecular Probes). Antibodies for western blotting: goat-anti-DDR2 (AF2538) was from R&D Systems (Abingdon, UK); mouse anti-phosphotyrosine, clone 4G10, from Upstate Biotechnology (Lake Placid, NY, USA); peroxidase-conjugated goat anti-human Fc from Jackson ImmunoResearch Laboratories (West Grove, PA, USA). Secondary antibodies for western blotting were as follows: rabbit-anti-goat Ig-horseradish peroxidase (Zymed Laboratories Inc., San Francisco, CA, USA); sheep-anti-mouse Ig-horseradish peroxidase (Amersham Biosciences UK, Chalfont St Giles, UK).

Isolation of genomic DNA

Genomic DNA was isolated from the peripheral blood leukocytes using Flexigene DNA Kit (Qiagen, GmbH) according to the manufacturer's instructions. DNA was dissolved in TE (Tris-EDTA) buffer and quantitated by spectrophotometry.

Polymerase chain reaction (PCR)

Exon-specific primers for *DDR2* gene (Supplementary Material, Table S1) were designed using Primer3 (http://frodo.wi.mit.edu/cgi-bin/primer3/) and used to amplify the coding exons 3–18 and their flanking regions. Amplification was carried out using 1U of *Taq* polymerase (Qiagen, GmbH), 0.2 mM of each of the dNTPs, 1× PCR reaction buffer, 1.5 mM $MgCl_2$, 5 pmol of each forward and reverse primers and 50 ng of genomic DNA template in 25 μl reactions. The PCR was performed by an initial 5 min denaturation at 95°C followed by 40 cycles of 95°C for 30 s, 58°C–62°C for 35 s and 72°C for 45 s with a final elongation at 72°C for 10 min.

DNA sequencing

Sequencing was performed using the dideoxy method by fluorescent automated sequencing on the ABI 3130*xl* genetic analyzer (Applied Biosystems, Foster City, CA, USA). The sequence data were analysed using Sequencing analysis software v5.3 (ABI, Foster City, CA, USA). Mutations are designated on the coding *DDR2* sequence with reference to GenBank accession number NM_001014796.1 with the A of the initiation codon ATG as number +1.

Protein expression vectors

Construction of the HA-tagged DDR2 construct. The HA-tagged version of the wild-type DDR2 was generated by sequential site-directed mutagenesis to introduce the nine amino acids of the HA tag (YPYDVPDYA) in two cycles using the pcDNA3.1-DDR2 plasmid (21) as a template. In the first cycle, we introduced five amino acids (YPYDV) of the HA tag prior to the stop codon of the DDR2 gene using the following mutagenesis primers.

HA1-F: CCACAAGGCGACGAG**TACCCATACGATGTT**TGATGCTGTCAGTGCC and HA1-R: GGCACTGACAGCATCA**AACATCGTATGGGTA**CTCGTCGCCTTGTGG. In the second cycle, the above construct was used as a template and the remaining four amino acids (PDYA) of the HA tag were introduced using the following mutagenesis primers. HA2-F: TACCCATACGATGTT**CCAGATTACGCT**TGATGCTGTCAGTGCC and HA2-R: GGCACTGACAGCATCA**AGCGTAATCTGG**AACATCGTATGGGTA.

Generation of missense DDR2 mutants. The missense mutants were introduced by QuickChange site-directed mutagenesis using Turbo *Pfu* polymerase (Stratagene) and using the untagged pcDNA3.1-DDR2 (21) and the C-terminally HA-tagged pcDNA3.1DDR2 as templates. The primers for the site-directed mutagenesis to introduce the missense mutations were as follows. DDR2-E113K-F: GAGGTCATGGCATC**A**AGTTTGCCCCCATG; DDR2-E113K-R: CATGGGGGCAAAC**T**TGATGCCATGACCTC; DDR2-T713I-F: CGAGATCTGGCCA**T**TCGAAACTGTTTAG; DDR2-T713I-R: CTAAACAGTTTCGA**A**TGGCCAGATCTCG; DDR2-I726-F: TACACAATCAAGA**G**AGCTGACTTTGGA; DDR2-I726R-R: TCCAAAGTCAGC**T**CTCTTGATTGTGTA; DDR2-R752C-F: GTGCTCCCTATC**T**GCTGGATGTCTTGG; DDR2-R752C-R: CCAAGACATCCA**G**CA**A**GATAGGGAGCAC.

Generation of E113K ectodomain construct tagged with human Fc. cDNA encoding E113K-DDR2 ectodomain (Lys22-Thr398) was obtained by PCR amplification and cloned into a modified pCEP-Pu vector containing a human Fc sequence, as described for the respective wild-type and W52A-DDR2 constructs (6).

All constructs were confirmed by direct DNA sequencing of the purified plasmids.

Cell culture and transfection

HeLa cells were cultured in Dulbecco's modified Eagle's medium (Invitrogen) supplemented with 10% fetal calf serum, 2 mM L-glutamine and 100 U/ml penicillin/streptomycin at 37°C with 10% CO_2. For transfection, cells were grown in 24 well tissue culture plates. Transfection was performed using the liposomal transfection reagent FuGENE 6 (Roche Biochemicals), according to manufacturer's instructions. A mixture of 1 μg of DDR2 wild-type or mutant plasmid DNA and 4 μl of FuGENE 6 in 94 μl of OPTIMEM I medium was applied to each well of the cultured cells. Twenty-four hours after transfection, the cells were fixed and processed for microscopy.

Human embryonic kidney (HEK) 293 cells (ATCC, Manassas, VA, USA) and HEK293-EBNA cells (Invitrogen Ltd., Paisley, UK) were cultured in Dulbecco's modified Eagle's medium/F12 medium (Invitrogen) supplemented with 10% fetal bovine serum, penicillin (10 U/ml) and streptomycin (100 μg/ml) at 37°C with 5% CO_2. For transfection, cells were grown in 24 well tissue culture plates (autophosphorylation assays) or 12 well tissue culture plates (deglycosylation assays) and were transfected with 1 or 2 μg, respectively, of DDR2 wild-type or mutant plasmid DNA using calcium phosphate precipitation.

Immunohistochemistry

For immunofluorescence, cover slip-grown HeLa cells were washed with phosphate-buffered saline (PBS), fixed by methanol at −20°C for 4 min. Fixed cells were washed in PBS three times then incubated in blocking solution (1% BSA in PBS) for 30 min at room temperature. The fixed cells were then incubated at room temperature for 1 h with either mouse monoclonal anti-HA antibody alone or co-stained with both mouse monoclonal anti-HA antibody and rabbit polyclonal anti-calnexin antibody. After washing with PBS, the cells were incubated with the appropriate secondary antibodies for 1 h at room temperature, washed several times with PBS and mounted in immuno fluor medium (ICN Biomedicals). Data were acquired using Leica DM-IRBE or Nikon confocal microscopes. For presentation, images were pseudocolored

as either red (DDR2) or green (calnexin and EGFP-H-Ras), contrast enhanced and overlayed using Adobe Photoshop® (Adobe Inc.). All images presented are single sections in the *z*-plane.

Deglycosylation assay

Forty hours after transfection, HEK293 cells were lysed in 1% Nonidet P-40, 150 mM NaCl, 50 mM Tris, pH 7.4, 1 mM EDTA, 1 mM phenylmethylsulfonyl fluoride, 50 μg/ml aprotinin. Twenty microliter of each cell lysate was denatured in 1X glycoprotein denaturing buffer (0.5% SDS and 1% β-mercaptoethanol) for 5 min at 100°C. The denatured lysates were then split into two equal aliquots which were incubated for 3 h at 37°C in the presence or absence of 10 U of Endoglycosidase H. Samples were then resolved on 7.5% SDS–PAGE followed by blotting onto nitrocellulose membranes and probing with anti-DDR2 antibodies, as described below.

Collagen-induced DDR2 autophosphorylation

The assay was performed as described previously in detail (21). Twenty-four hours after transfection, HEK293 cells were incubated with serum-free medium for 16 h. Cells were then stimulated with collagen I (2–50 μg/ml) for 90 min at 37°C. Cells were lysed in 1% Nonidet P-40, 150 mM NaCl, 50 mM Tris, pH 7.4, 1 mM EDTA, 1 mM phenylmethylsulfonyl fluoride, 50 μg/ml aprotinin, 1 mM sodium orthovanadate and 5 mM NaF. Aliquots of the lysates were analyzed by SDS–PAGE followed by blotting onto nitrocellulose membranes. The duplicate blots were probed with either anti-phosphotyrosine monoclonal antibody or anti-DDR2 antibodies followed by corresponding horseradish peroxidise-conjugated secondary antibodies. Detection was performed using Enhanced Chemiluminescence Plus (Amersham Biosciences) and an Ettan DIGE Imager (GE Healthcare Biosciences).

Production and purification of recombinant proteins

The production and purification of recombinant DDR2 proteins was essentially as previously described (6,21). The recombinant Fc-tagged wild-type and E113K-DDR2 extracellular domain proteins were isolated from episomally transfected HEK293-EBNA cells and purified by affinity chromatography on a HiTrap rProtein A column (17-5079-01, GE Healthcare Biosciences, Uppsala, SW, USA) using an ÄKTA™ Purifier (GE Healthcare Biosciences). Both proteins were obtained in similar yields (4.0 mg per liter of conditioned medium for wild-type DDR2, 3.5 mg per liter of conditioned medium for E113K-DDR2).

Solid-phase collagen binding assays

The assay procedure has been described previously in detail (21). Briefly, rat tail collagen I or bovine collagen II was diluted in 50 mM Tris pH 7.5, 100 mM NaCl to 10 μg/ml and coated onto Maxisorp 96-well plates (Fisher Scientific) overnight at room temperature. Wells were then blocked for 1 h at room temperature with 1 mg/ml bovine serum albumin in phosphate-buffered saline plus 0.05% Tween-20. Recombinant Fc-tagged wild-type or mutant DDR2 extracellular domain proteins, diluted in incubation buffer (0.5 mg/ml bovine serum albumin in phosphate-buffered saline plus 0.05% Tween 20), were added for 3 h at room temperature. Wells were then washed six times with incubation buffer. Bound Fc-tagged DDR2 proteins were then detected with goat anti-human Fc coupled to horseradish peroxidase (1:3333 dilution), added for 1 h at room temperature followed by six washes with incubation buffer. A color reaction was subsequently performed using o-phenylenediamine dihydrochloride (Sigma), added for 3–5 min. The reaction was stopped with 3 M H_2SO_4, and plates were read at 492 nm on a 96-well plate reader.

SUPPLEMENTARY MATERIAL

Supplementary Material is available at *HMG* online.

ACKNOWLEDGEMENTS

We would like to thank the patients and their families for taking part in this study. We are especially grateful to Prof Erhard Hohenester for providing Figure 8. We also like to thank Dr Alistair Hume for his help and comments and Mr Saeed Tariq for his help with confocal imaging.

Conflict of Interest statement. The authors declare that there are no conflicts of interest in this study.

FUNDING

This work was supported by the Dubai Harvard Foundation for Medical Research (grant number 2008-04 to B.R.A. and L.A.); and the UK Medical Research Council (G0701121 to B.L.). Funding to pay the Open Access publication charges for this article was provided by MRC grant G0701121.

REFERENCES

1. Vogel, W., Gish, G.D., Alves, F. and Pawson, T. (1997) The discoidin domain receptor tyrosine kinases are activated by collagen. *Mol. Cell*, **1**, 13–23.
2. Shrivastava, A., Radziejewski, C., Campbell, E., Kovac, L., McGlynn, M., Ryan, T.E., Davis, S., Goldfarb, M.P., Glass, D.J., Lemke, G. *et al.* (1997) An orphan receptor tyrosine kinase family whose members serve as nonintegrin collagen receptors. *Mol. Cell*, **1**, 25–34.
3. Leitinger, B., Steplewski, A. and Fertala, A. (2004) The D2 period of collagen II contains a specific binding site for the human discoidin domain receptor, DDR2. *J. Mol. Biol.*, **344**, 993–1003.
4. Leitinger, B. and Kwan, A.P. (2006) The discoidin domain receptor DDR2 is a receptor for type X collagen. *Matrix Biol.*, **25**, 355–364.
5. Noordeen, N.A., Carafoli, F., Hohenester, E., Horton, M.A. and Leitinger, B. (2006) A transmembrane leucine zipper is required for activation of the dimeric receptor tyrosine kinase DDR1. *J. Biol. Chem.*, **281**, 22744–22751.
6. Carafoli, F., Bihan, D., Stathopoulos, S., Konitsiotis, A.D., Kvansakul, M., Farndale, R.W., Leitinger, B. and Hohenester, E. (2009) Crystallographic insight into collagen recognition by discoidin domain receptor 2. *Structure*, **17**, 1573–1581.
7. Vogel, W.F., Abdulhussein, R. and Ford, C.E. (2006) Sensing extracellular matrix: an update on discoidin domain receptor function. *Cell. Signal.*, **18**, 1108–1116.

8. Leitinger, B. and Hohenester, E. (2007) Mammalian collagen receptors. *Matrix Biol.*, **26**, 146–155.
9. Labrador, J.P., Azcoitia, V., Tuckermann, J., Lin, C., Olaso, E., Manes, S., Bruckner, K., Goergen, J.L., Lemke, G., Yancopoulos, G. *et al.* (2001) The collagen receptor DDR2 regulates proliferation and its elimination leads to dwarfism. *EMBO Rep.*, **2**, 446–452.
10. Kano, K., Marin de Evsikova, C., Young, J., Wnek, C., Maddatu, T.P., Nishina, P.M. and Naggert, J.K. (2008) A novel dwarfism with gonadal dysfunction due to loss-of-function allele of the collagen receptor gene, Ddr2, in the mouse. *Mol. Endocrinol.*, **22**, 1866–1880.
11. Bargal, R., Cormier-Daire, V., Ben-Neriah, Z., Le Merrer, M., Sosna, J., Melki, J., Zangen, D.H., Smithson, S.F., Borochowitz, Z., Belostotsky, R. *et al.* (2009) Mutations in DDR2 gene cause SMED with short limbs and abnormal calcifications. *Am. J. Hum. Genet.*, **84**, 80–84.
12. Borochowitz, Z., Langer, L.O. Jr, Gruber, H.E., Lachman, R., Katznelson, M.B. and Rimoin, D.L. (1993) Spondylo-meta-epiphyseal dysplasia (SMED), short limb-hand type: a congenital familial skeletal dysplasia with distinctive features and histopathology. *Am. J. Med. Genet.*, **45**, 320–326.
13. Langer, L.O. Jr, Wolfson, B.J., Scott, C.I. Jr, Reid, C.S., Schidlow, D.V., Millar, E.A., Borns, P.F., Lubicky, J.P. and Carpenter, B.L. (1993) Further delineation of spondylo-meta-epiphyseal dysplasia, short limb-abnormal calcification type, with emphasis on diagnostic features. *Am. J. Med. Genet.*, **45**, 488–500.
14. Afzal, A.R. and Jeffery, S. (2003) One gene, two phenotypes: ROR2 mutations in autosomal recessive Robinow syndrome and autosomal dominant brachydactyly type B. *Hum. Mutat.*, **22**, 1–11.
15. Chen, Y., Bellamy, W.P., Seabra, M.C., Field, M.C. and Ali, B.R. (2005) ER-associated protein degradation is a common mechanism underpinning numerous monogenic diseases including Robinow syndrome. *Hum. Mol. Genet.*, **14**, 2559–2569.
16. Ali, B.R., Jeffery, S., Patel, N., Tinworth, L.E., Meguid, N., Patton, M.A. and Afzal, A.R. (2007) Novel Robinow syndrome causing mutations in the proximal region of the frizzled-like domain of ROR2 are retained in the endoplasmic reticulum. *Hum. Genet.*, **122**, 389–395.
17. Al-Gazali, L.I., Bakalinova, D. and Sztriha, L. (1996) Spondylo-meta-epiphyseal dysplasia, short limb, abnormal calcification type. *Clin. Dysmorphol.*, **5**, 197–206.
18. Aridor, M. and Hannan, L.A. (2000) Traffic jam: a compendium of human diseases that affect intracellular transport processes. *Traffic*, **1**, 836–851.
19. Aridor, M. (2007) Visiting the ER: the endoplasmic reticulum as a target for therapeutics in traffic related diseases. *Adv. Drug Deliv. Rev.*, **59**, 759–781.
20. Hume, A.N., Buttgereit, J., Al-Awadhi, A.M., Al-Suwaidi, S.S., John, A., Bader, M., Seabra, M.C., Al-Gazali, L. and Ali, B.R. (2009) Defective cellular trafficking of missense NPR-B mutants is the major mechanism underlying acromesomelic dysplasia-type Maroteaux. *Hum. Mol. Genet.*, **18**, 267–277.
21. Leitinger, B. (2003) Molecular analysis of collagen binding by the human discoidin domain receptors, DDR1 and DDR2. Identification of collagen binding sites in DDR2. *J. Biol. Chem.*, **278**, 16761–16769.
22. Konitsiotis, A.D., Raynal, N., Bihan, D., Hohenester, E., Farndale, R.W. and Leitinger, B. (2008) Characterization of high affinity binding motifs for the discoidin domain receptor DDR2 in collagen. *J. Biol. Chem.*, **283**, 6861–6868.
23. Ichikawa, O., Osawa, M., Nishida, N., Goshima, N., Nomura, N. and Shimada, I. (2007) Structural basis of the collagen-binding mode of discoidin domain receptor 2. *EMBO J.*, **26**, 4168–4176.
24. Green, J.L., Kuntz, S.G. and Sternberg, P.W. (2008) Ror receptor tyrosine kinases: orphans no more. *Trends Cell Biol.*, **18**, 536–544.
25. Hampton, R.Y. (2002) Proteolysis and sterol regulation. *Annu. Rev. Cell Dev. Biol.*, **18**, 345–378.
26. Romisch, K. (2004) A cure for traffic jams: small molecule chaperones in the endoplasmic reticulum. *Traffic*, **5**, 815–820.
27. Sayeed, A. and Ng, D.T. (2005) Search and destroy: ER quality control and ER-associated protein degradation. *Crit. Rev. Biochem. Mol. Biol.*, **40**, 75–91.
28. Nakatsukasa, K. and Brodsky, J.L. (2008) The recognition and retrotranslocation of misfolded proteins from the endoplasmic reticulum. *Traffic*, **9**, 861–870.
29. Anelli, T. and Sitia, R. (2008) Protein quality control in the early secretory pathway. *EMBO J.*, **27**, 315–327.
30. Aridor, M. and Hannan, L.A. (2002) Traffic jams II: an update of diseases of intracellular transport. *Traffic*, **3**, 781–790.
31. Fano, V., Lejarraga, H. and Barreiro, C. (2001) Spondylo-meta-epiphyseal dysplasia, short limbs, abnormal calcification type: a new case with severe neurological involvement. *Pediatr. Radiol.*, **31**, 19–22.
32. Dias, C., Cairns, R. and Patel, M.S. (2009) Sudden death in spondylo-meta-epiphyseal dysplasia, short limb-abnormal calcification type. *Clin. Dysmorphol.*, **18**, 25–29.
33. Tuysuz, B., Gazioglu, N., Ungur, S., Aji, D.Y. and Turkmen, S. (2009) The time of onset of abnormal calcification in spondylometaepiphyseal dysplasia, short limb-abnormal calcification type. *Pediatr. Radiol.*, **39**, 84–89.
34. Smithson, S.F., Grier, D. and Hall, C.M. (2009) Spondylo-meta-epiphyseal dysplasia, short limb-abnormal calcification type. *Clin. Dysmorphol.*, **18**, 31–35.